Atmos. Chem. Phys. Discuss., doi:10.5194/acp-2016-1133, 2017
Manuscript under review for journal Atmos. Chem. Phys.
Published: 2 January 2017

Atmospheric Chemistry and Physics Discussions

Photochemical aging of organic and inorganic ambient aerosol from the Potential Aerosol Mass (PAM) reactor experiment in East Asia

Eunha Kang[1,2], Meehye Lee[1], William H. Brune[3], Taehyoung Lee[4], Joonyoung Ahn[5]

[1]Department of Earth and Environmental Sciences, Korea University, Republic of Korea

[2]Department of Urban and Environmental studies, Suwon Research Institute, Republic of Korea

[3]Department of Meteorology, Pennsylvania State University, USA

[4]Department of Environmental Science, Hankuk University of Foreign Studies, Republic of Korea

[5]National Institute of Environmental Research, Republic of Korea

[1] Corresponding author, meehye@korea.ac.kr

Atmos. Chem. Phys. Discuss., doi:10.5194/acp-2016-1133, 2017
Manuscript under review for journal Atmos. Chem. Phys.
Published: 2 January 2017

Atmospheric Chemistry and Physics Discussions

Abstract

We investigated the photochemical aging of ambient aerosols using a potential aerosol mass (PAM) reactor at Baengnyeong Island in the Yellow Sea during August 4–12, 2011. The size distributions and chemical compositions of the ambient and aged PAM aerosols were measured alternately every 6 min by Scanning Mobility Particle Sizer (SMPS) and High Resolution-Time of Flight-Aerosol Mass Spectrometer (HR-ToF-AMS), respectively. Inside the PAM reactor, the O_3 and OH levels were equivalent to approximately 5 days of integrated OH exposure at typical atmospheric conditions. Two types of air masses were distinguished on the basis of the chemical composition and the degree of aging: Sulfate was predominant with higher O:C ratio for the air transported from China and organic concentration was higher than that of sulfate with lower O:C ratio when the air came through the Korean Peninsula. In PAM reactor, sulfate was constantly formed, resulting in the increase of particle mass at 200–400 nm size range. Organics were responsible for an overall loss of mass in 100–200 nm particles. This loss was especially evident for the m/z 43 component representing semi-volatile organics. Conversely, the m/z 44 component corresponding to low-volatile organics increased with a shift toward larger sizes during the organics-dominated episode. Therefore, we hypothesize that the oxidation of semi-volatile organics was facilitated by gas-phase oxidation and partitioning for re-equilibrium between the gas and particle phases. Nitrate evaporated in the PAM reactor upon the addition of sulfate to the particles. These results suggest that the chemical composition of aerosols and their degree of photochemical aging particularly for organics are also crucial in determining aerosol mass concentrations. Because sulfate in the atmosphere was stable for about a week of the nominal lifetime of aerosols, SO_2 is a unquestionably primary precursor of secondary aerosol in northeast Asia. In comparison, the contribution of organics to secondary aerosols is more variable during transport in the atmosphere. Notably, an increase in low-volatility organics was associated with sulfate and evident at 200–400 nm, highlighting the role of secondary organic aerosol (SOA) in cloud condensation nuclei (CCN) formation.

Atmos. Chem. Phys. Discuss., doi:10.5194/acp-2016-1133, 2017
Manuscript under review for journal Atmos. Chem. Phys.
Published: 2 January 2017

Atmospheric Chemistry and Physics Discussions

1. Introduction

In East Asia, atmospheric aerosols are a cause of public concern because of the frequent occurrence of haze in mega cities and industrial areas and dust storms in deserts and extremely dry regions, and their transboundary transport (Takami et al., 2007; Wu et al., 2009; Kim et al., 2009; Ramana et al., 2010; Kang et al., 2013). These occurrences impact the regional air quality and climate (Li et al., 2011; Huang et al., 2014). Aerosol plumes are able to remain in the atmosphere for up to 10 days and can be transported across the Pacific Ocean. During transport, air masses become photochemically aged, leading to the generation of secondary aerosols and subsequent modification of the optical and microphysical properties of aerosols (Dunlea et al., 2009; Lim et al., 2014). This transformation process has been studied by collecting ambient air across the Pacific Ocean or by tracking the Asian plumes onboard aircrafts (Brock et al., 2004; Aggarwal and Kawamura, 2009; Dunlea et al., 2009; Peltier et al., 2008).

Secondary aerosols (SA) comprise inorganics such as sulfate and nitrate as well as organics. Of these, secondary organic aerosols (SOA) are of more interest because they are produced in the atmosphere from numerous organic species and are aged through complex mechanisms, during which their physicochemical properties such as volatility, hygroscopicity, and optical properties are altered. The absorption and scattering properties of aerosols in northeast Asia was reported to be intimately linked with their chemical composition (Lim et al., 2014). As aerosols are oxidized, the hygroscopicity of organic aerosols (OAs) increases, suggesting photochemically driven CCN activation of SOA (Massoli et al., 2010; Lambe et al., 2011; King et al., 2010; Morgan et al., 2010).

To understand SOA formation and aging processes, experiments have been conducted using environmental chambers (Kroll and Seinfeld, 2008; Hallquist et al., 2009). In these large environmental chambers, atmospheric simulations are limited to the equivalent of only about a day, which is much shorter than the nominal lifetime of aerosols, which is around a week. In addition, ambient air masses are under influence of

Atmos. Chem. Phys. Discuss., doi:10.5194/acp-2016-1133, 2017
Manuscript under review for journal Atmos. Chem. Phys.
Published: 2 January 2017

Atmospheric Chemistry and Physics Discussions

various emissions and mixing processes, which are not properly represented in these well-mixed and long-residence time chambers (Jimenez et al., 2009; Ng et al., 2010).

Thus, we introduced the potential aerosol mass (PAM) chamber, a continuous flow reactor under high levels of OH and O_3, which is applicable for both controlled lab studies and ambient air (Kang et al., 2007; Kang et al., 2011b; Massoli et al., 2010; Lambe et al., 2012; Cubison et al., 2011). The highly oxidizing conditions of the PAM reactor are suitable for examining SOA formation and oxidation processes for the equivalent of a week (Jimenez et al., 2009; George and Abbatt, 2010). In particular, the PAM reactor is not vulnerable to wall losses, which are significant for conventional chambers. Thus, PAM reactor is able to reasonably simulate aging processes of SOA after formation (Kang et al., 2011a). In the first field deployment of PAM in northeast Asia, Kang et al. (2011) reported PAM simulation results for different air masses and demonstrated that oxidation processes occurring in the natural atmosphere were plausibly integrated in the PAM reactor.

In this study, we deployed a PAM reactor at an island site in the Yellow Sea to investigate the photochemical aging processes of ambient aerosols in the northeast Asia. Their size, mass, chemical, and transformation characteristics were thoroughly examined with a particular emphasis on SOA formation and transformation.

2. Experimental methods

Experiments were conducted at a measurement station on Baengnyeong Island in the Yellow Sea (37.967°N, 124.630°E, 100 m asl) from August 4 to August 12, 2011 (Fig. 1a). As the northernmost and westernmost part of South Korea, Baengnyeong Island is located 740 km west of Beijing and 211 km east of Seoul. The measurement station was established by the National Institute of Environmental Research (NIER) as a core background site of the National Monitoring Network to observe Asian dust transported from China.

Atmos. Chem. Phys. Discuss., doi:10.5194/acp-2016-1133, 2017
Manuscript under review for journal Atmos. Chem. Phys.
Published: 2 January 2017

Atmospheric Chemistry and Physics Discussions

Ambient air collected using a PM1.0 cyclone was pulled through the PAM chamber for 6 minutes, during which time the ambient aerosols were oxidized (hereafter referred to as "PAM aerosols"). For another 6 minutes, the ambient air was directly pumped into the analytical instruments, bypassing the PAM chamber. The ambient and PAM aerosols were alternately measured every 6 minutes thereafter, producing pseudo-simultaneous measurements. The chemical composition of aerosol was measured by a high-resolution time-of-flight aerosol mass spectrometer (HR-ToF-AMS, hereafter referred to as "AMS") and their number concentration was determined in the mobility diameter range of 10.4–469.8 nm with a scanning mobility particle sizer (SMPS 3034, TSI). The aerosol mass concentration was obtained from the volume concentration multiplied by an assumed particle density of 1.2 g cm^{-3}. Detailed descriptions of the HR-ToF-AMS and the sampling site can be found elsewhere (Lee et al., 2015).

The potential aerosol mass (PAM) reactor is a small flow-through aluminum cylinder equipped with long Hg lamps to produce large amounts of OH and O_3, creating a highly oxidizing environment. Detailed descriptions of the PAM reactors are given in previous publications (Kang et al., 2007; Kang et al., 2011b; Lambe et al. 2011). The PAM reactor employed in this study is the same version as that described in Lambe et al. (2011), which was also used for laboratory studies of SOA aging (Lambe et al. 2012; 2015). Inside the PAM reactor, the OH exposure was approximately 7 x 10^{11} molecules cm^{-3} s, which is equivalent to an integrated OH concentration over 5 days at a typical noon-time concentration of 1.5x10^{6} molecules cm^{-3}. The OH exposure was calibrated against sulfur dioxide decay (Kang et al., 2011a).

In previous laboratory experiments using this version of the PAM reactor, air was pulled through 1-cm diameter tubing into the enclosed reactor and rapidly dispersed before entering the chamber through a Silconert-coated (Silcotech, Inc.) stainless steel screen. In the present study, the tubing and the endcap were removed so that ambient air was brought directly through the screen into the chamber. In this configuration, the wall-

Atmos. Chem. Phys. Discuss., doi:10.5194/acp-2016-1133, 2017
Manuscript under review for journal Atmos. Chem. Phys.
Published: 2 January 2017

Atmospheric Chemistry and Physics Discussions

loss of aerosol particles was found to be negligible, enabling quantitative comparison between the ambient and PAM aerosols.

For ambient air, sulfur dioxide (SO_2), nitrogen dioxide (NO_2), carbon monoxide (CO), ozone (O_3), PM_{10} mass, elemental carbon (EC), and organic carbon (OC) were simultaneously measured, along with meteorological parameters (Table 1). The HYSPLIT backward trajectory model, which was developed by the National Oceanic and Atmospheric Administration (NOAA), was used to examine the history of the sampled air masses.

3. Results

3.1. Measurement overview of ambient and PAM aerosols

Aerosol mass concentrations varied from 0.5 to 38 μg m^{-3} for both the PAM aerosols and the ambient aerosols (Fig. 2a) during the entire experiment period. Although the PAM aerosol masses were generally greater than the ambient aerosol masses, the former was occasionally less than the latter. The difference in mass concentrations between the PAM aerosols and the ambient aerosols was in the range of ~3–7 μg m^{-3}, indicating that photo-oxidation resulted either in the loss of pre-existing particles or in the formation of secondary aerosols.

Particle mass distributions of the ambient and PAM aerosols were averaged for the entire experiment and their difference is presented in Figure 3. In the PAM chamber, nuclei-mode particles were formed (average dN/dlogDp = 2 x 10^5 cm^{-3}) but their contribution to the total aerosol mass was relatively insignificant due to their small sizes of less than 50 nm in diameter (Dp). In comparison, the mass of PAM aerosol was distinctively increased at larger size than 200 nm. Particles between 50 and 200 nm in diameter were variably lost or produced in the PAM reactor, depending on the history of the air masses.

Major species compositions including sulfate, organics, ammonium, and nitrate for

Atmos. Chem. Phys. Discuss., doi:10.5194/acp-2016-1133, 2017
Manuscript under review for journal Atmos. Chem. Phys.
Published: 2 January 2017

Atmospheric Chemistry and Physics Discussions

both ambient and PAM aerosols are presented in Figure 2b. In general, sulfate and ammonium concentrations were generally higher or lower in the PAM reactor compared to ambient air depending on the air masses. In contrast, total organics and nitrate were always lower in the PAM aerosols relative to ambient aerosols.

3.2. Organics- and sulfate-dominated episodes

Throughout the experiment, ambient aerosols were highly enhanced during two separate periods (shaded in Fig. 2a), with distinct differences in chemical composition between the two. While the ambient air was enriched in organics during the first episode (August 6, 11 AM to August 7, 9 AM), sulfate was dominant in the second episode (August 9, 1 AM to August 9, 6 PM). During the two episodes, the levels of gaseous precursors including NOx, SO_2, and CO were higher than in the remaining periods (Fig. 4). However, the ratios of both SO_2/NOx and OC/EC were higher for the first case than the second case. It was opposite for O_3/CO ratios. These two cases were distinguished by the air masses (Fig. 1b). Higher concentrations of organics than sulfate during the first episode resulted from air that had passed through the Korean Peninsula. The sulfate-dominated air in the second episode had been transported from Southeast China. In addition, the air mass trajectories imply that sulfate-dominated aerosols lingered over the Yellow Sea and were aged more than the organics-dominated aerosols.

In addition, the aerosol masses differed in terms of size distributions between the two episodes (Fig. 5). The mass difference between the ambient and PAM aerosols (gain and loss) was greater in all size ranges for the organics-dominated episode than the sulfate-dominated episode. In the PAM reactor, the mass of particles smaller than 50 nm and larger than 200 nm increased, but it decreased in the size range of 100–200 nm.

The measurement results of size-separated chemical compositions provide detailed information on transformation processes in the PAM reactor. In general, sulfate increased

Atmos. Chem. Phys. Discuss., doi:10.5194/acp-2016-1133, 2017
Manuscript under review for journal Atmos. Chem. Phys.
Published: 2 January 2017

but total organics and nitrate were reduced in the PAM reactor compared to the ambient aerosols (Fig. 6). The contribution of ammonium ions to the total mass was also greatest when aerosols were enriched in sulfate. The organic m/z 43 and m/z 44 components exhibited different behavior in the PAM reactor between the two episodes (Fig. 5). While m/z 43 decreased in the PAM reactor in both episodes, m/z 44 only increased during the sulfate-dominated episode.

Therefore, the following discussion is focused on these two distinct aerosols episodes, for which the size-separated chemical compositions were thoroughly examined and compared in order to elaborate on the formation of secondary aerosols and the evolution of ambient aerosols upon photo-oxidation in the PAM reactor.

4. Discussion

4.1. Formation of nuclei-mode particles

In the current study, the formation of nuclei-mode particles (Dp <50 nm) was always observed in the PAM reactor. SO_2 is primarily responsible for the formation of new nuclei mode particles. In previous field studies, increases in the amounts of PAM aerosols were dependent on the ambient SO_2 concentrations (Kang et al., 2013). For the two episodes in this study, the number concentrations of nuclei-mode particles differed by less than an order of magnitude and SO_2 concentrations were similar. Chemical compositions are not available for nuclei-mode particles due to an AMS cut-off size of 50 nm in the present study. Additionally, VOC concentrations for ambient air were not determined. In a previous controlled lab experiment, nuclei-mode particles were produced from single VOC and SO_2 gas in a PAM reactor (Kang et al., 2011b). Although the formation mechanism is not fully understood, non-linear oscillatory nucleation likely occurs during a burst of

Atmos. Chem. Phys. Discuss., doi:10.5194/acp-2016-1133, 2017
Manuscript under review for journal Atmos. Chem. Phys.
Published: 2 January 2017

Atmospheric Chemistry and Physics Discussions

gaseous oxidation reactions in the presence of large amounts of oxidants. Therefore, the nucleation of tiny clusters from photo-oxidation of VOCs as well as SO_2 possibly took place under the highly oxidative conditions produced by large amounts of OH and O_3.

4.2. Formation and evolution of organic aerosols

The SMPS mass size distributions highlight the size range of 100~200 nm, where PAM aerosol was reduced in mass only for organics-dominated episode (Fig. 5). The AMS mass size distribution showed that the ambient Semi-Volatile Oxygenated Organic Aerosols (SV-OOAs) were mostly found in the range of 100–200 nm Dp and Low-Volatile Oxygenated Organic Aerosols (LV-OOAs) greater than 200 nm (Mohr et al., 2012). In addition, the semi-volatile organics were known to be easily oxidized to organics with lower volatility in the PAM chamber (Kang et al., 2011). These results suggest that there were less oxidized OAs (e.g., SV-OOAs) more in the organics-dominated than the sulfate-dominated episode. The ratios of O:C were lower for organics-dominated aerosols than those of sulfate-dominated aerosols (Fig. 7). In conjunction with O:C ratio, the air mass trajectories (Fig. 1b) imply organics-dominated air masses were relatively less aged thereby, including more SV-OOAs than those of the sulfate-dominated episode (Jimenez et al., 2009; Ng et al., 2011).

The AMS measurement results indicate that total organics and the organic m/z 43 component were consistently reduced in the PAM reactor. Possible loss mechanisms are the deposition of aerosols on the chamber wall (McMurry and Grosjean, 1985; La et al., 2016) and fragmentation reactions from further photo-oxidation to form products with higher vapor pressure (Lamb et al., 2012). The wall loss of aerosols was not considered in this study, because the PAM reactor used in this study was modified with passivated conductive material to minimize the electrostatic loss of aerosols and increase the particle transmission efficiency, especially for ambient aerosols (Lambe et al., 2011). It was also

Atmos. Chem. Phys. Discuss., doi:10.5194/acp-2016-1133, 2017
Manuscript under review for journal Atmos. Chem. Phys.
Published: 2 January 2017

Atmospheric Chemistry and Physics Discussions

demonstrated that sulfate and ammonium were not lost in the PAM reactor. For the entire experiment, the O:C ratios of PAM aerosols were greater than those of ambient aerosols, with O:C ratios corresponding to SV-OOAs and LV-OOAs (Jimenez et al., 2009). Thus, a chemical transformation from low O:C to high O:C is more likely to explain the organic mass loss.

Organics are known to be oxidized by OH undergoing functionalization and fragmentation. The pathway by which this occurs is determined by the oxidation state of the existing organic aerosols. Functionalization dominates in the early stage of oxidation, which increases total organics and organic m/z 43, while fragmentation dominates in the later stage of oxidation, reducing OA mass (Jimenez et al., 2009; Kroll et al., 2009; Chacon-Madrid et al., 2010; Henry and Donahue, 2012; Lambe et al., 2012). For highly oxidized OAs with O:C ratios greater than 0.4, fragmentation becomes especially dominant, resulting in OA mass loss. In this study, the measured O:C ratios of the ambient aerosols were greater than 0.4 for both episodes (Fig. 7), which indicates that the observed ambient organic aerosols were aged enough to be fragmented. Figure 7 demonstrates that the Van Krevelen slope (Δ(H:C)/ Δ(O:C)) became steeper in the higher O:C ratio range for the organic-rich case. In a laboratory PAM experiment, Lambe et al. (2012) observed a similar tendency and explained that as SOA oxidized, the Van Krevelen slope changed from minor fragmentation of carbonyl and acids/alcohol formation to major fragmentation of acids formation. In the present study, therefore, fragmentation is thought to play a major role in the loss of organics.

In comparison, the organic m/z 44 mass increased in PAM aerosols for the organics-dominated episode but not for the sulfate-dominated episode. In particular, the increase in organic m/z 44 mass was associated with larger sizes than the organic m/z 43 mass loss (Fig. 6). As mentioned above, organic m/z 43 loss was significant for sizes less than 200 nm in AMS diameter, but most of the increase in organic m/z 44 mass was observed in the size greater than 200 nm. If particles grew in size by heterogeneous

Atmos. Chem. Phys. Discuss., doi:10.5194/acp-2016-1133, 2017
Manuscript under review for journal Atmos. Chem. Phys.
Published: 2 January 2017

Atmospheric Chemistry and Physics Discussions

oxidation of carbonyls to carboxylic acids on pre-existing particle surfaces, the mass decrease in m/z 43 should also have been associated with an increase in the m/z 44 mass by the addition of oxygen in the sulfate-dominated episode. During the sulfate-dominated episode, however, there was no difference in the organic m/z 44 mass between the ambient and PAM aerosols, implying that a gas-phase reaction in the photo-chemical oxidation of organic aerosols was involved. Thus, the mass increase of the m/z 44 component in PAM aerosols was considered in terms of gas-to-particle partitioning.

Upon being aged, OAs are formed not only from precursor gaseous phases but are also evaporated by partitioning between gas and aerosol phases. The evaporated OAs possibly undergo chemical oxidation, being partitioned into aerosol phase again. Therefore, SOAs can form from the oxidation of evaporated primary OAs as well as VOCs and Intermediate VOCs (Donahue et al., 2009). The organics-dominated episode of this study was characterized by higher organic concentrations and higher OC/EC ratios compared to the sulfate-dominated episode, which implies the availability of primary OAs and relatively less loss by aging or greater SOA formation, compared to photo-chemically inert EC.

The oxidation of organics in the atmosphere can occur both in the gas phase and through heterogeneous reactions. The gas-phase reaction is tens of times faster than the heterogeneous reaction, being limited by diffusion to the particle surface (Lambe et al., 2012). In our experiment, it was not feasible to distinguish gas-phase oxidation of semi-volatile organics in equilibrium with the particle phase from heterogeneous oxidation of organics on the particle surface. Nonetheless, the main result of this study demonstrates that a distinct loss in m/z 43 was accompanied by little change in m/z 44, which supports the possibility that gas-phase oxidation was involved in SOA formation. The distributions of m/z 43-like compounds such as carbonyl groups with a semi-volatile nature in gaseous and particulate phases are controlled by the partitioning equilibrium between the two phases. In contrast, m/z 44-like compounds such as organic acid groups with low volatility tend to preferentially remain in the particle phase (Ng et al., 2011). It is, therefore, quite

Atmos. Chem. Phys. Discuss., doi:10.5194/acp-2016-1133, 2017
Manuscript under review for journal Atmos. Chem. Phys.
Published: 2 January 2017

likely to occur in PAM reactor that the gas-phase concentration of m/z 43-like compounds was decreased by further oxidation and fragmentation, leading to evaporation of organic m/z 43 in particle phase to be re-equilibrated with the decreased concentration in gas phase. On the other hand, m/z 44-like compounds were sufficiently less volatile that they underwent little evaporation to the gas phase. Thus, the probability that they participated in heterogeneous oxidation was relatively low. In the PAM reactor, the residence time on the order of ~100 s rendered gas-phase reactions efficient, but possibly limited the extent of slower heterogeneous oxidation (Lambe et al., 2012). It was also found in a previous study that much less OA mass loss occurred for highly oxidized OAs with low volatility than in less oxidized OAs due to heterogeneous oxidation (Kessler et al., 2012). In addition to the loss of less oxidized organics (m/z 43), the AMS measurements indicated that highly oxidized OAs (m/z 44) were produced in the PAM reactor. In particular, the m/z 44 peak was found to occur in the same size range as that of sulfate. These results suggest that SOAs formed by gas-phase oxidation and subsequent condensation on the surface of existing sulfate particles. Indeed, robust evidence for this can be found in detailed laboratory studies of SOA formation on acidic seed particles (Jang et al., 2002; Jang et al., 2006; Kang et al., 2007)

In the present study, the overall mass spectra of organics indicate significant loss of less oxidized OAs (e.g., m/z 41, 42, 43, ...) in the PAM reactor for both episodes. In addition, CO^+ and COO^+ groups increased and decreased in the PAM aerosols for the organics-dominated and sulfate-dominated episodes, respectively (Fig. 5). Therefore, the discussion on single mass of organic m/z 43 and m/z 44 will also be valid for the entire organic classes.

4.3. Formation and evolution of inorganic aerosols

In the PAM aerosols, sulfate concentrations were always greater than or similar to

Atmos. Chem. Phys. Discuss., doi:10.5194/acp-2016-1133, 2017
Manuscript under review for journal Atmos. Chem. Phys.
Published: 2 January 2017

Atmospheric Chemistry and Physics Discussions

those of the ambient aerosols for the entire experiment period. This indicates a significant contribution of sulfate to secondary aerosols in the PAM reactor, in which sulfuric acid was produced through photo-oxidation of SO_2 under high OH exposure and then nucleated or was deposited on pre-existing particles (Kang et al., 2007). For the two selected cases especially, sulfate mass was noticeably increased in condensation mode where the condensation of gas on particle surfaces would be favored, particularly under highly oxidative conditions. Although nuclei-mode particles increased in number to a great extent, their mass contribution was insignificant at the ambient level of gaseous precursors. In this study, the variation in ammonium concentrations was similar to that of sulfate (Fig. 2b). In addition, the equivalent ratios of sulfate and nitrate to ammonium indicated that the particles were neutral or acidic, depending on the air masses. The aerosol was neutralized by formation of an ammonium salt and thus the condensation-mode sulfate was likely to exist as ammonium sulfate.

In the organics-dominated episode, the increase of the PAM aerosol mass in particles larger than 200 nm resulted from the formation of sulfate and organic m/z 44 as described earlier (Fig. 5 & 6), in which sulfate exhibited a broad peak in 200–500 nm particles, as in ambient air. In comparison, the sulfate increase shifted toward smaller sizes in the 200–400 nm range during the sulfate-dominated episode, leading to a sharp peak at 200 nm. Unlike the organics-dominated episode, the loss of organic m/z 43 was not accompanied by an increase in organic m/z 44 during the sulfate-dominated episode. The loss of organic m/z 43 was observed in smaller size than the increase in organic m/z 44 was observed. These features resulted in the difference in overall mass distributions between the two episodes shown in Fig. 5

For organics-dominated episode, the aerosol mass was decreased at 100-200 nm in PAM reactor, of which particles seemed to grow in size into the condensation mode by the addition of sulfuric acid formed from the oxidation of SO_2. This then implies that photo-oxidation efficiently activates organic particles to become cloud condensation-mode

Atmos. Chem. Phys. Discuss., doi:10.5194/acp-2016-1133, 2017
Manuscript under review for journal Atmos. Chem. Phys.
Published: 2 January 2017

particles under SO_2-sufficient conditions. In addition, an increase in sulfate mass was noticeable between 200–400 nm. A major inorganic constituent, nitrate was lost in the PAM reactor during both episodes, with an ambient nitrate concentration that was comparable to the levels of sulfate and organics (Fig. 2b). The nitrate loss is rather explicit in the PAM reactor because of efficient conversion of SO_2 to sulfate, causing the aerosols to become acidic and causing particulate nitrate (HNO_3(p)) to evaporate. A plausible source of HNO_3(p) in the PAM reactor is the deposition of gaseous HNO_3(g) and heterogeneous reaction of NO_2 on the particle surfaces. If a particle is acidic in the presence of sulfuric acids, nitrate easily evaporates back to the gas phase. In the organics-dominated episode, the equivalent ratio of ambient aerosol ($[NH_4]/(2x[SO_4]+[NO_3])$ was 1.0 and sulfate increased significantly in the PAM reactor. Although the equivalent ratio of the ambient aerosol was 0.7 during the sulfate-dominated event, sulfate was further increased in the PAM reactor. However, the PAM aerosol became less acidic due to an equivalent loss of nitrate over the condensation mode and because the nitrate mode shifted toward larger sizes. These results illustrate the role of sulfate in determining chemical compositions and mass loadings of aerosols in northeast Asia.

4.4. Atmospheric implications

The ambient OAs in the present study were moderately to well aged, as indicated by their O:C ratios greater than 0.4. They were chemically and physically transformed in the PAM reactor, resulting in increased O:C ratios and decreased OA mass concentrations by photochemical oxidation and fragmentation processes. Although the oxidant levels of OH and O_3 in the PAM reactor far exceeded the ambient levels, the H:C and O:C ratios of the ambient and PAM OAs were in close agreement with those observed in the atmosphere (Ng et al., 2011) (Fig. 7). These results provide good evidence for the ability of the PAM reactor to accelerate oxidation processes in ambient air under high O_3 and OH conditions and to represent atmospheric aging of approximately 5 days without physical

Atmos. Chem. Phys. Discuss., doi:10.5194/acp-2016-1133, 2017
Manuscript under review for journal Atmos. Chem. Phys.
Published: 2 January 2017

367 removal processes such as dry/wet deposition. It further confirms that the PAM reactor is
368 applicable for field studies to observe aging processes of various types of precursors and
369 aerosols including emissions sources and long-range transported air masses.

370 The O:C ratios of OAs from this study were plotted against aging time and
371 compared with those observed in East Asia (Fig. 8), where the O:C ratios were found to
372 increase with transport time across the Pacific Ocean (Takegawa et al., 2006; Takami et al.,
373 2007; Dunlea et al., 2009). The O:C ratios of the bulk OAs depend on the concentrations of
374 organic constituents because the saturation vapor pressure varies with the molecular
375 weight of the organics (Donahue et al., 2006). Thus, the O:C ratios from different studies
376 are not directly comparable if their OAs concentrations vary within a wide range. In Figure
377 8, OA concentrations ranged up to 10 μg m^3 and thus a comparison among different sets
378 of measurements is suitable. It is noteworthy that the increase in O:C ratios with
379 photochemical aging was slightly higher in our results than in those of previous studies,
380 which was probably due to fragmentation during the transition in oxidation state.

381 The results of this study imply that SO_2 plays a key role in increasing secondary
382 aerosol concentrations in East Asia because the lifetime of SO_2 is longer than those of
383 VOCs and because sulfate is relatively stable in the particle phase once formed, contrary to
384 nitrate and organics. While SOA formation is more important near sources or in fresh air
385 masses, OAs oxidation occurs continuously during the transport of air masses. In particular,
386 this study proposes that relatively less aged OAs were in equilibrium with the gas phase,
387 through which oxidation of SV-OOAs was carried out, leading to increased OA mass in the
388 CCN size range (200–400 nm). The increased O:C ratios rendered particles more
389 hygroscopic, thereby facilitating their activation as CCNs (Massoli et al., 2010). Thus,
390 climate effect of OA aging should be considered along with deceases in OA mass loading
391 when they are transported across long distances.

392

Atmos. Chem. Phys. Discuss., doi:10.5194/acp-2016-1133, 2017
Manuscript under review for journal Atmos. Chem. Phys.
Published: 2 January 2017

Atmospheric Chemistry and Physics Discussions

5. Conclusions

A PAM reactor was used to analyze ambient air at Baegnyeong Island in the northern part of the Yellow Sea during August 4–12, 2011. The chemical compositions and number concentrations of ambient and PAM aerosols were alternately determined with ToF-AMS and SMPS, respectively. The integrated OH exposure was equivalent to 5 days of atmospheric photo-oxidation. The results of the present study demonstrate that the high levels of OH and O_3 in the PAM reactor can expedite slow atmospheric reactions and that chemical aging processes of the natural atmosphere are plausibly represented.

During the experiment, two periods of noticeably enhanced aerosol concentrations with different chemical compositions and degrees of air mass aging were observed. While organic concentrations were highest during August 6–7 and sulfate was more elevated on August 9, the ratio of O:C was higher for the latter than the former. In addition, the size-dependent mass distributions of major constituents were clearly distinguished between the two episodes, which were used to understand the photochemical and volatile properties of the aerosols.

In the PAM chamber, sulfate formed in condensation mode in particle sizes between 200 and 400 nm and presumably in nucleation mode for particles smaller than 50 nm, which suggests that SO_2 was not limited in the study region for generating secondary aerosols, even during summer. In contrast, nitrate was lost in particles of all size ranges due to evaporation by the addition of sulfate. The total mass of organics was reduced in particles between 100 and 400 nm, where the loss in the m/z 43 component was evident for both episodes. In contrast, the more oxidized organic m/z 44 component was produced at larger sizes of 200–400 nm only during the organics-dominated episode. These results suggest partitioning of SV-OOA into a gas-phase that was in equilibrium with the particle phases. As the concentration of SV-OOA decreased upon its oxidation and fragmentation in gas-phase, it evaporated away from the particle phase in the process of re-equilibration.

Atmos. Chem. Phys. Discuss., doi:10.5194/acp-2016-1133, 2017
Manuscript under review for journal Atmos. Chem. Phys.
Published: 2 January 2017

421 As the air mass aged, the loss was apparent for photochemically and physically
422 unstable component such as organics and nitrate, whereas sulfate was stable in the
423 aerosol phase. Therefore, organics and nitrate are likely to be relatively more important in
424 near-source regions while sulfate is probably dominant in areas far from the source. The
425 results highlight the importance of chemical composition and oxidation processes in
426 determining the aerosol-forming power of an air mass. Although organic mass
427 concentrations decreased with photochemical aging, OAs were transformed from SV-OOAs
428 to LV-OOAs, as demonstrated by an increase in the organic m/z 44 component at sizes of
429 200–400 nm where sulfate was consistently increased. In conjunction with the increased
430 O:C ratio of organics, this underscores the potential of organics to act as cloud
431 condensation nuclei under SO_2-sufficient conditions.

432

433 **Acknowledgement**

434

435 This study was supported by the Korea Meteorological Administration Research
436 and Development Program under Grant KMIPA 2015-6020 and the National Research
437 Foundation of Korea (NRF) through the Basic Science Research Program (NRF-2011-355-
438 c00174).

Atmos. Chem. Phys. Discuss., doi:10.5194/acp-2016-1133, 2017
Manuscript under review for journal Atmos. Chem. Phys.
Published: 2 January 2017

Atmospheric Chemistry and Physics Discussions

439 Table 1. Meteorological parameters and measurement summary for organics-dominated
440 and sulfate-dominated episodes.

	Organics-dominated (Aug. 6, 11 AM~ Aug. 7, 9 AM)		**Sulfate-dominated** (Aug. 9, 1 AM~ Aug. 9, 2 PM*)	
Meteorological parameters				
Temp(℃)	26 ± 0.8		20 ± 0.6	
Relative humidity (%)	84 ± 7.7		96 ± 0.2	
Wind speed (m/s)	5 ± 1.6		8 ± 1.7	
Wind direction	easterly		southwesterly	
Weather mark	Cloudy		Fog	
	Gaseous species			
SO_2 (ppbv)	3.1 ± 0.3		3.4 ± 0.2	
NO_2 (ppbv)	2.4 ± 0.8		0.9 ± 0.3	
CO (ppmv)	0.2 ± 0.0		0.4 ± 0.1	
O_3 (ppbv)	46 ± 22		54 ± 8	
Aerosol species[#]				
	Ambient	**PAM**	**Ambient**	**PAM**
Mass[&]	14.0 ± 4.5	16.3 ± 5.1	24.3 ± 6.5	26.6 ± 7.6
Sulfate	1.43 ± 0.63	2.12 ± 0.88	6.07 ± 2.30	6.59 ± 2.24
Nitrate	0.72 ± 0.47	0.32 ± 0.12	0.88 ± 0.54	0.22 ± 0.10
Ammonium	0.77 ± 0.33	0.96 ± 0.33	2.01 ± 0.67	2.01 ± 0.66
Organics	5.05 ± 1.73	3.45 ± 1.21	2.22 ± 0.77	1.29 ± 0.39
m/z 43	0.34 ± 0.10	0.15 ±0.04	0.11 ± 0.04	0.04 ± 0.01
m/z 44	0.75 ± 0.30	0.91 ± 0.34	0.47 ± 0.17	0.43 ± 0.12

441 * Data from 9 AM to 12 AM, August 9 were excluded because of rain.
442 # Units are μg cm^{-3}.
443 [&] Aerosol mass concentrations were obtained from SMPS measurements with an aerosol density of
444 1.2 μg cm^{-3} and sulfate, nitrate, ammonium and organics were from HR-ToF-AMS measurements.
445

Atmos. Chem. Phys. Discuss., doi:10.5194/acp-2016-1133, 2017
Manuscript under review for journal Atmos. Chem. Phys.
Published: 2 January 2017

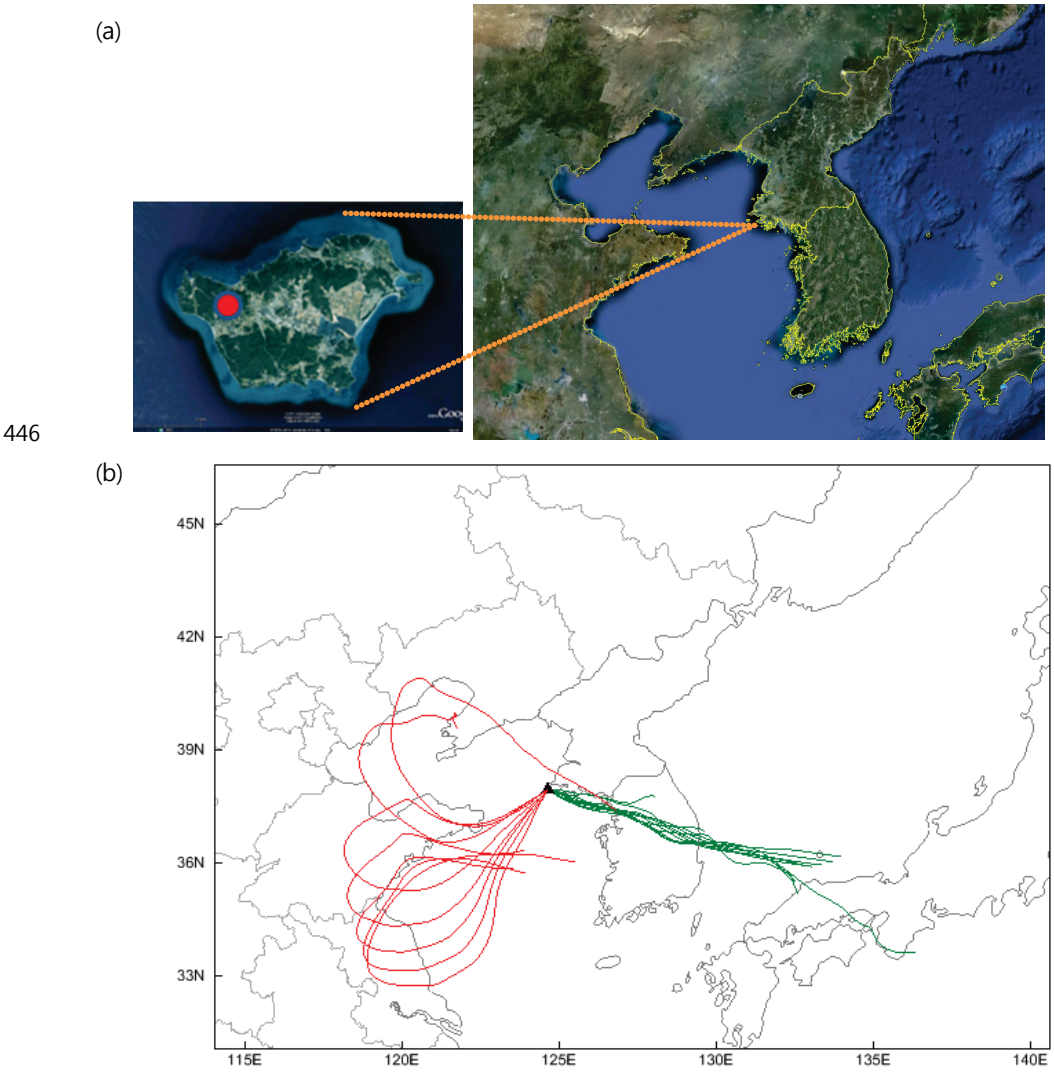

Figure 1. (a) The location of the measurement site on Baengnyeong Island, the northernmost island in South Korea. The red circle indicates the measurement station location. (b) 72-hour backward trajectory for the two episodes. Green represents the organics-dominated episode during August 6, 11 AM to August 7, 9 AM, 2011, while red represents the sulfate-dominated episode during August 9, 1 AM to August 9, 2 PM, 2011.

Atmos. Chem. Phys. Discuss., doi:10.5194/acp-2016-1133, 2017
Manuscript under review for journal Atmos. Chem. Phys.
Published: 2 January 2017

Atmospheric Chemistry and Physics Discussions

(a)

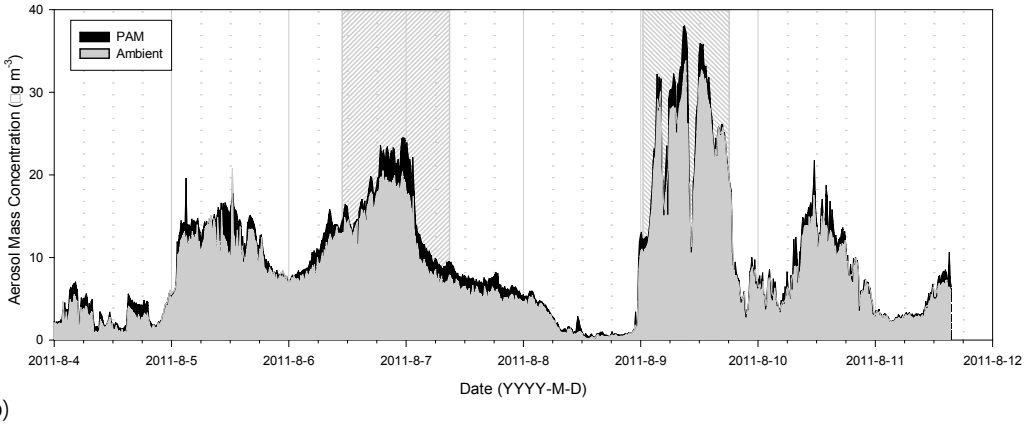

(b)

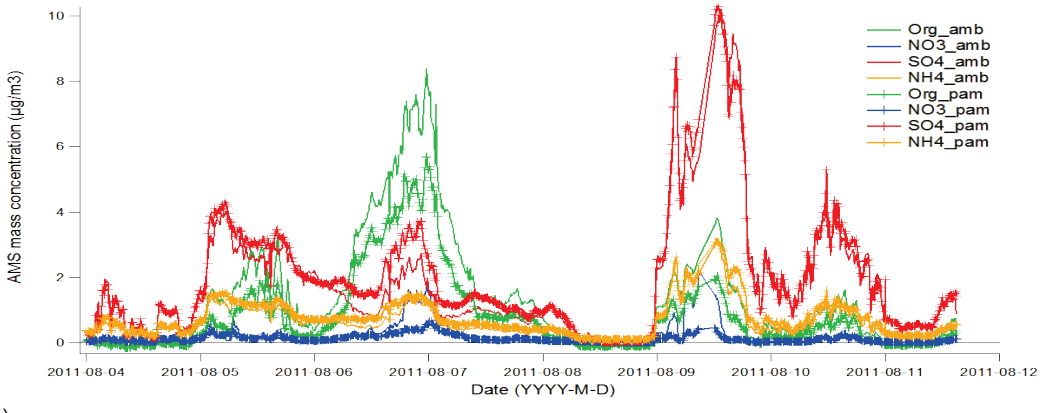

(c)

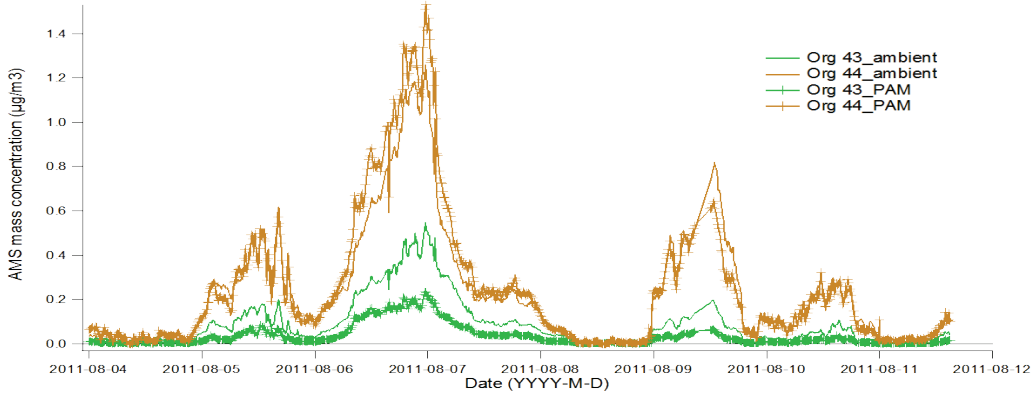

Atmos. Chem. Phys. Discuss., doi:10.5194/acp-2016-1133, 2017
Manuscript under review for journal Atmos. Chem. Phys.
Published: 2 January 2017

Atmospheric Chemistry and Physics Discussions

459 Figure 2. Time series of experimental results. Shaded periods represent the organics-
460 dominated episode (August 6, 11 AM to August, 7 9 AM) and the sulfate-
461 dominated episode (August 9, 1 AM to August 9, 2 PM). The lowest mass
462 concentration observed on August 8 was due to rain. (a) Aerosol mass
463 concentrations from SMPS measurements for ambient and PAM aerosols. (b) Mass
464 concentrations of major components measured by HR-ToF-AMS including organics,
465 nitrate, sulfate, ammonium, and organic m/z 43 and m/z 44 m. Solid lines and
466 lines with markers represent ambient aerosols and PAM aerosols, respectively.

Atmos. Chem. Phys. Discuss., doi:10.5194/acp-2016-1133, 2017
Manuscript under review for journal Atmos. Chem. Phys.
Published: 2 January 2017

Atmospheric Chemistry and Physics Discussions

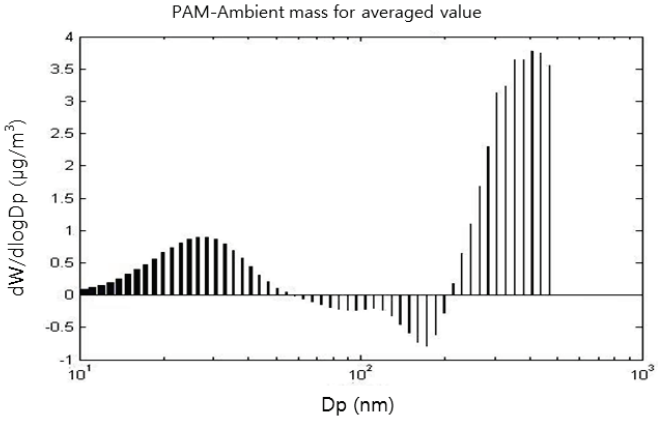

467

468

469 Figure 3. SMPS mass difference between PAM and ambient aerosols averaged for the
470 entire sampling period.

Atmos. Chem. Phys. Discuss., doi:10.5194/acp-2016-1133, 2017
Manuscript under review for journal Atmos. Chem. Phys.
Published: 2 January 2017

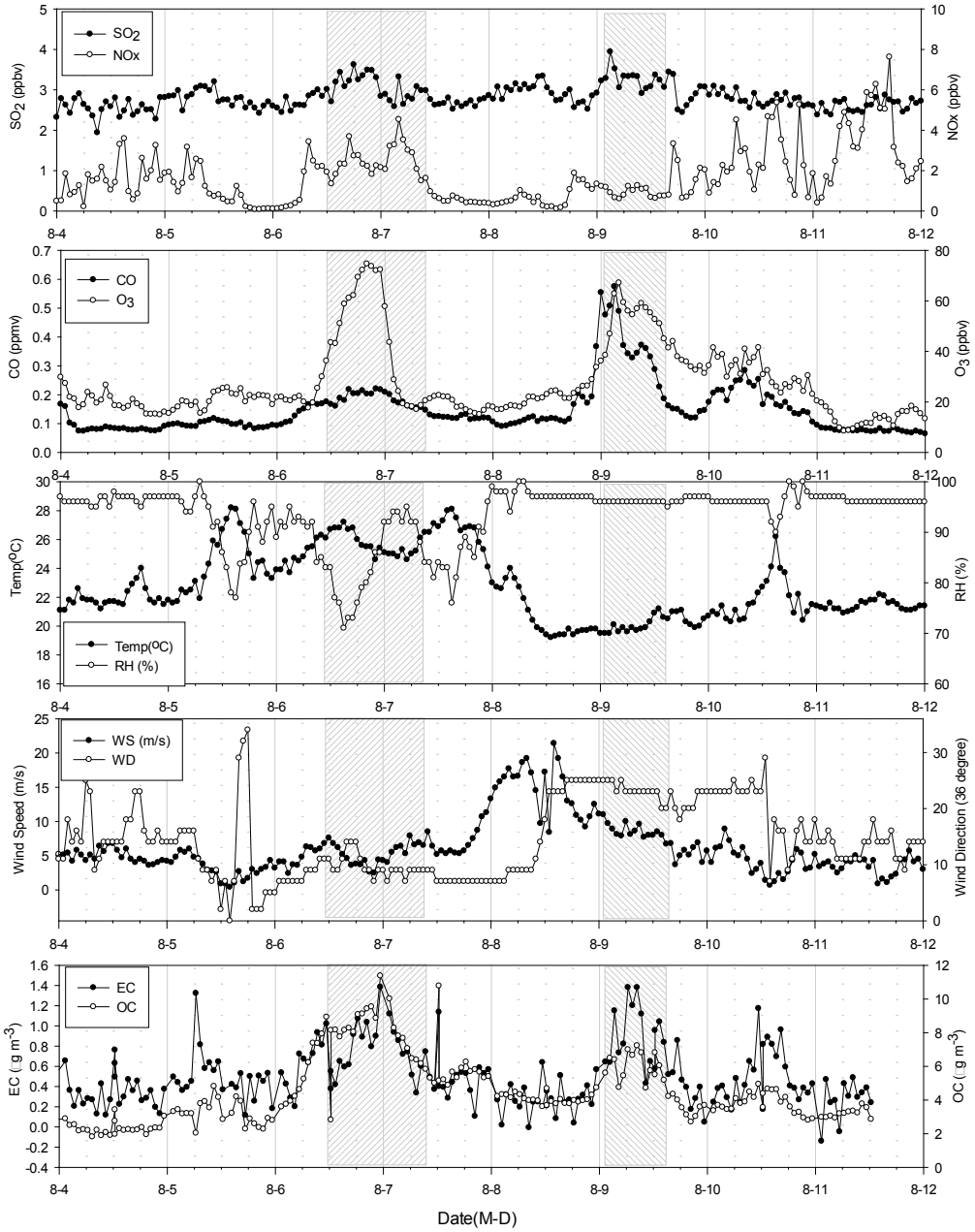

Figure 4. Hourly measurements of SO_2, NOx, CO, O_3, and meteorological parameters for the entire sampling period.

Atmos. Chem. Phys. Discuss., doi:10.5194/acp-2016-1133, 2017
Manuscript under review for journal Atmos. Chem. Phys.
Published: 2 January 2017

Atmospheric Chemistry and Physics Discussions

474 (a)

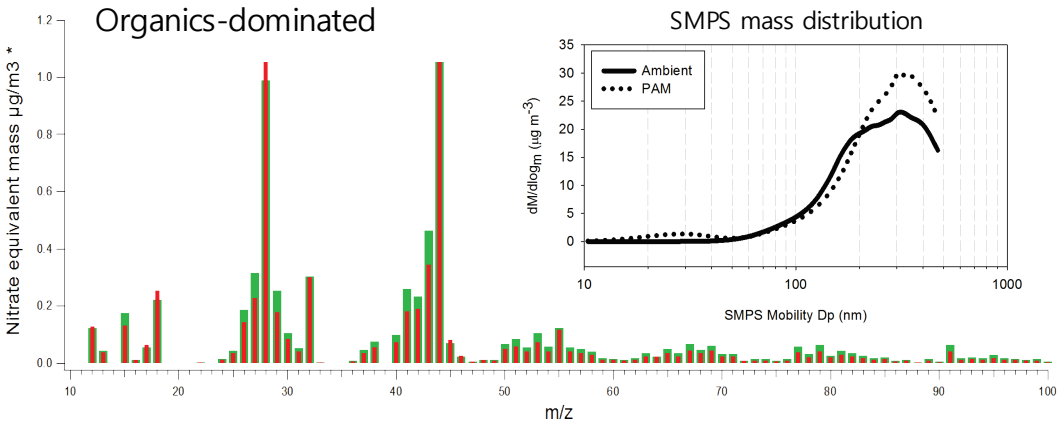

475

476

477 (b)

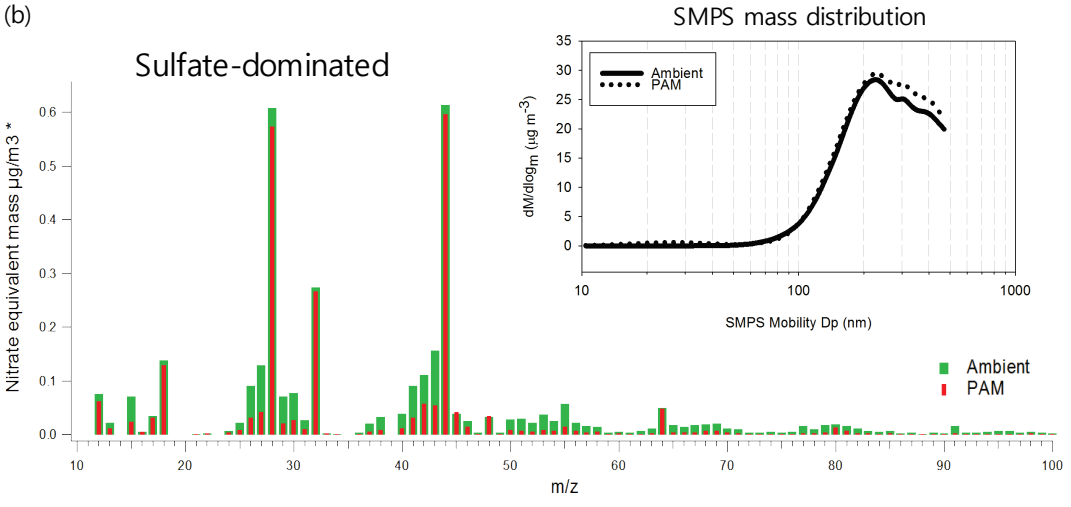

478

479

480 Figure 5. AMS mass spectra of organics and SMPS mass size distribution averaged for
481 (a) organics-dominated episode and (b) sulfate-dominated episode.

Atmos. Chem. Phys. Discuss., doi:10.5194/acp-2016-1133, 2017
Manuscript under review for journal Atmos. Chem. Phys.
Published: 2 January 2017

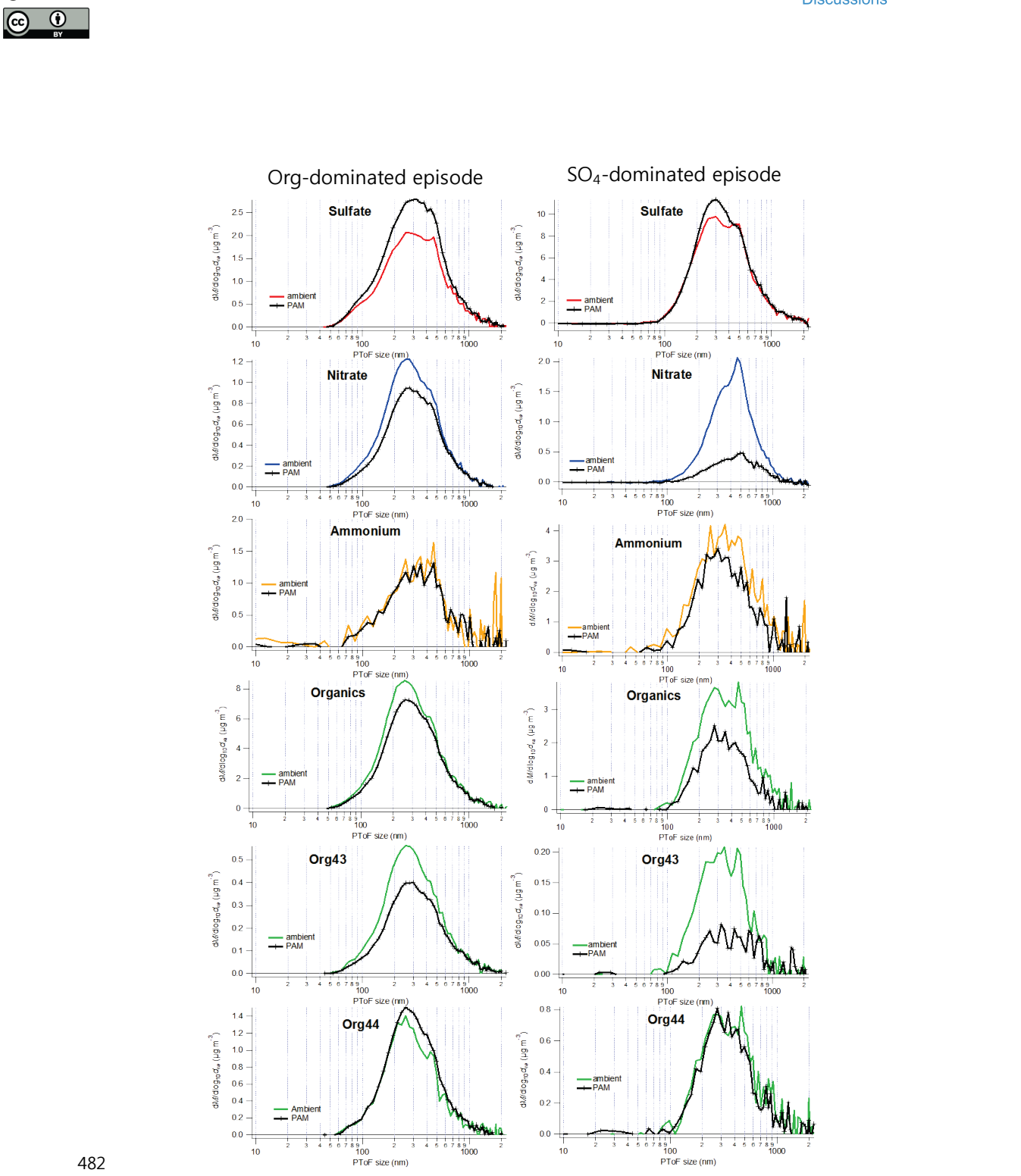

Figure 6. AMS p-ToF size distributions of PAM and ambient aerosol components averaged for organics- and sulfate-dominated episode.

Atmos. Chem. Phys. Discuss., doi:10.5194/acp-2016-1133, 2017
Manuscript under review for journal Atmos. Chem. Phys.
Published: 2 January 2017

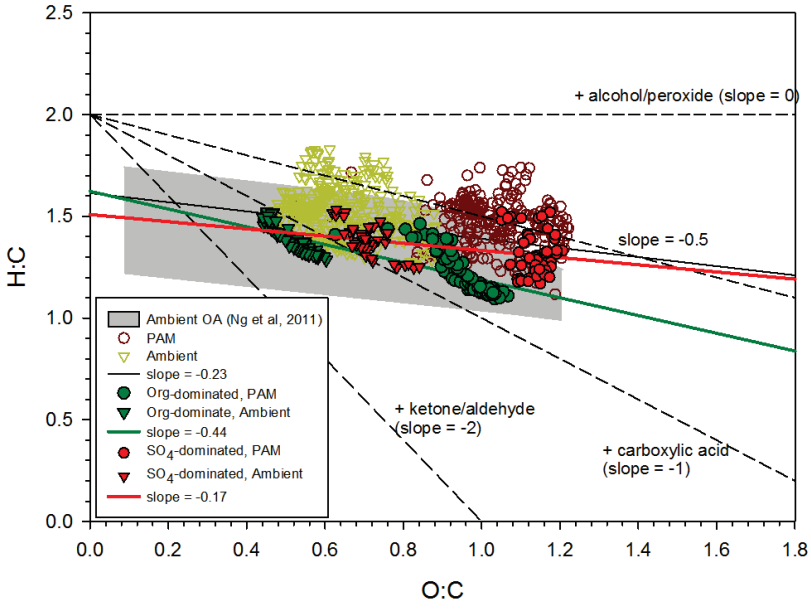

485

486 Figure 7. Van Krevelen diagram for the entire sampling period and two episodes. Dashed
487 lines represent the Van Krevelen slopes, Δ(H:C)/ Δ(O:C) to show the direction of
488 particular functional group additions (Heald et al., 2010). Shaded gray areas
489 represent the H:C and O:C ranges observed in ambient OAs (Ng et al., 2011).

Atmos. Chem. Phys. Discuss., doi:10.5194/acp-2016-1133, 2017
Manuscript under review for journal Atmos. Chem. Phys.
Published: 2 January 2017

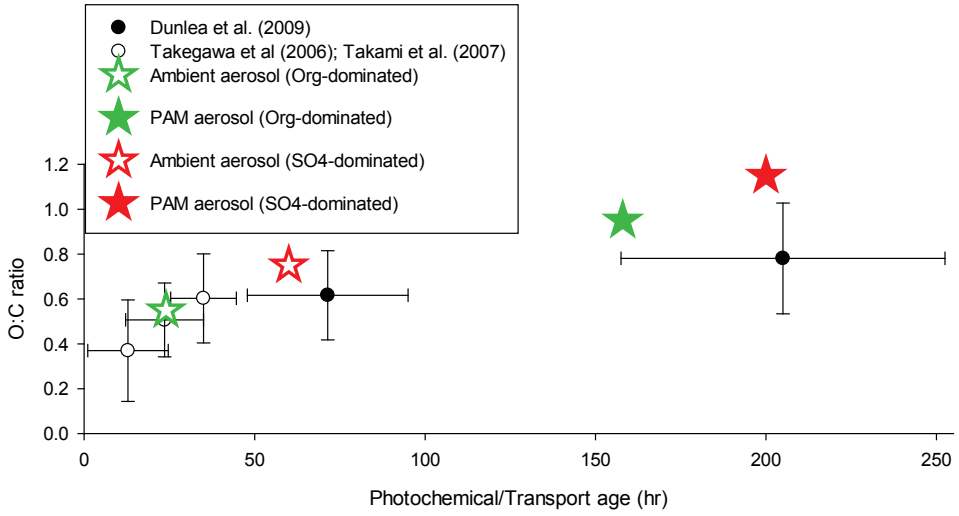

Figure 8. Comparison of O:C ratios in this study and other studies with respect to photochemical age. The photochemical ages in our measurement were obtained by the transport time calculated from a back trajectory analysis and photochemical aging times in the PAM chamber. Other study data were obtained from Takegawa et al. (2006), Takami et al. (2007), and Dunlea et al. (2009).

Atmos. Chem. Phys. Discuss., doi:10.5194/acp-2016-1133, 2017
Manuscript under review for journal Atmos. Chem. Phys.
Published: 2 January 2017

Atmospheric Chemistry and Physics Discussions

References

Aggarwal, S. G., and Kawamura, K.: Carbonaceous and inorganic composition in long-range transported aerosols over northern Japan: Implication for aging of water-soluble organic fraction, Atmospheric Environment, 43, 2532-2540, 2009.

Andreae, M. O., and Gelencser, A.: Black carbon or brown carbon? The nature of light-absorbing carbonaceous aerosols, Atmos Chem Phys, 6, 3131-3148, 2006.

Bateman, A. P., Nizkorodov, S. A., Laskin, J., and Laskin, A.: Photolytic processing of secondary organic aerosols dissolved in cloud droplets, Physical Chemistry Chemical Physics, 13, 12199-12212, Doi 10.1039/C1cp20526a, 2011.

Brock, C. A., Hudson, P. K., Lovejoy, E. R., Sullivan, A., Nowak, J. B., Huey, L. G., Cooper, O. R., Cziczo, D. J., de Gouw, J., Fehsenfeld, F. C., Holloway, J. S., Hubler, G., Lafleur, B. G., Murphy, D. M., Neuman, J. A., Nicks, D. K., Orsini, D. A., Parrish, D. D., Ryerson, T. B., Tanner, D. J., Warneke, C., Weber, R. J., and Wilson, J. C.: Particle characteristics following cloud-modified transport from Asia to North America, J Geophys Res-Atmos, 109, Artn D23s26 Doi 10.1029/2003jd004198, 2004.

Chacon-Madrid, H. J., Presto, A. A., and Donahue, N. M.: Functionalization vs. fragmentation: n-aldehyde oxidation mechanisms and secondary organic aerosol formation, Physical Chemistry Chemical Physics, 12, 13975-13982, Doi 10.1039/C0cp00200c, 2010.

Cubison, M. J., Ortega, A. M., Hayes, P. L., Farmer, D. K., Day, D., Lechner, M. J., Brune, W. H., Apel, E., Diskin, G. S., Fisher, J. A., Fuelberg, H. E., Hecobian, A., Knapp, D. J., Mikoviny, T., Riemer, D., Sachse, G. W., Sessions, W., Weber, R. J., Weinheimer, A. J., Wisthaler, A., and Jimenez, J. L.: Effects of aging on organic aerosol from open biomass burning smoke in aircraft and laboratory studies, Atmos Chem Phys, 11, 12049-12064, DOI 10.5194/acp-11-12049-2011, 2011.

Donahue, N. M., Robinson, A. L., Stanier, C. O., and Pandis, S. N.: Coupled partitioning, dilution, and chemical aging of semivolatile organics, Environ Sci Technol, 40, 2635-2643, Doi 10.1021/Es052297c, 2006.

Dunlea, E. J., DeCarlo, P. F., Aiken, A. C., Kimmel, J. R., Peltier, R. E., Weber, R. J., Tomlinson, J., Collins,

525 D. R., Shinozuka, Y., McNaughton, C. S., Howell, S. G., Clarke, A. D., Emmons, L. K., Apel, E. C., Pfister,
526 G. G., van Donkelaar, A., Martin, R. V., Millet, D. B., Heald, C. L., and Jimenez, J. L.: Evolution of Asian
527 aerosols during transpacific transport in INTEX-B, Atmos Chem Phys, 9, 7257-7287, 2009.

528 George, I. J., and Abbatt, J. P. D.: Chemical evolution of secondary organic aerosol from OH-initiated
529 heterogeneous oxidation, Atmos Chem Phys, 10, 5551-5563, DOI 10.5194/acp-10-5551-2010, 2010.

530 Hallquist, M., Wenger, J. C., Baltensperger, U., Rudich, Y., Simpson, D., Claeys, M., Dommen, J.,
531 Donahue, N. M., George, C., Goldstein, A. H., Hamilton, J. F., Herrmann, H., Hoffmann, T., Iinuma, Y.,
532 Jang, M., Jenkin, M. E., Jimenez, J. L., Kiendler-Scharr, A., Maenhaut, W., McFiggans, G., Mentel, T. F.,
533 Monod, A., Prevot, A. S. H., Seinfeld, J. H., Surratt, J. D., Szmigielski, R., and Wildt, J.: The formation,
534 properties and impact of secondary organic aerosol: current and emerging issues, Atmos Chem
535 Phys, 9, 5155-5236, 2009.

536 Heald, C. L., Kroll, J. H., Jimenez, J. L., Docherty, K. S., DeCarlo, P. F., Aiken, A. C., Chen, Q., Martin, S.
537 T., Farmer, D. K., and Artaxo, P.: A simplified description of the evolution of organic aerosol
538 composition in the atmosphere, Geophys Res Lett, 37, Artn L08803, Doi 10.1029/2010gl042737,
539 2010.

540 Henry, K. M., and Donahue, N. M.: Photochemical Aging of alpha-Pinene Secondary Organic Aerosol:
541 Effects of OH Radical Sources and Photolysis, J. Phys. Chem. A, 116, 5932-5940, Doi
542 10.1021/Jp210288s, 2012.

543 Huang, R.J., Zhang, Y., Bozzetti, C., Ho, K.F., Cao, J.J., Han, Y., Daellenbach, K.R., Slowik, J.G., Platt,
544 S.M., Canonaco, F., Zotter, P., Wolf, R., Pieber, S.M., Bruns, E.A., Crippa, M., Ciarelli, G., Piazzalunga, A.,
545 Schwikowski, M., Abbaszade, G., Schnelle-Kreis, J., Zimmermann, R., An, Z., Szidat, S., Baltensperger,
546 U., Haddad, I.E., and Prevot, A.S.H.: High secondary aerosol contribution to particulate pollution
547 during haze events in China, Nature, 514, 218-222, 2014.

548 Jang, M., Czoschke, N. M., Northcross, A. L., Cao, G., and Shaof, D.: SOA formation from partitioning
549 and heterogeneous reactions: Model study in the presence of inorganic species, Environ Sci Technol,
550 40, 3013-3022, Doi 10.1021/Es0511220, 2006.

551 Jang, M. S., Czoschke, N. M., Lee, S., and Kamens, R. M.: Heterogeneous atmospheric aerosol
552 production by acid-catalyzed particle-phase reactions, Science, 298, 814-817, DOI
553 10.1126/science.1075798, 2002.

554 Jimenez, J. L., Canagaratna, M. R., Donahue, N. M., Prevot, A. S. H., Zhang, Q., Kroll, J. H., DeCarlo, P.
555 F., Allan, J. D., Coe, H., Ng, N. L., Aiken, A. C., Docherty, K. S., Ulbrich, I. M., Grieshop, A. P., Robinson,
556 A. L., Duplissy, J., Smith, J. D., Wilson, K. R., Lanz, V. A., Hueglin, C., Sun, Y. L., Tian, J., Laaksonen, A.,
557 Raatikainen, T., Rautiainen, J., Vaattovaara, P., Ehn, M., Kulmala, M., Tomlinson, J. M., Collins, D. R.,
558 Cubison, M. J., Dunlea, E. J., Huffman, J. A., Onasch, T. B., Alfarra, M. R., Williams, P. I., Bower, K.,
559 Kondo, Y., Schneider, J., Drewnick, F., Borrmann, S., Weimer, S., Demerjian, K., Salcedo, D., Cottrell, L.,
560 Griffin, R., Takami, A., Miyoshi, T., Hatakeyama, S., Shimono, A., Sun, J. Y., Zhang, Y. M., Dzepina, K.,
561 Kimmel, J. R., Sueper, D., Jayne, J. T., Herndon, S. C., Trimborn, A. M., Williams, L. R., Wood, E. C.,
562 Middlebrook, A. M., Kolb, C. E., Baltensperger, U., and Worsnop, D. R.: Evolution of Organic Aerosols
563 in the Atmosphere, Science, 326, 1525-1529, DOI 10.1126/science.1180353, 2009.

564 Kang, E., Root, M. J., Toohey, D. W., and Brune, W. H.: Introducing the concept of Potential Aerosol
565 Mass (PAM), Atmos Chem Phys, 7, 5727-5744, 2007.

566 Kang, E., Brune, W. H., Kim, S., Yoon, S. C., Jung, M., and Lee, M.: A preliminary PAM measurement
567 of ambient air at Gosan, Jeju to study the secondary aerosol forming potential, Journal of Korean
568 Society for Atmospheric Environment, 27, 11, 2011a.

569 Kang, E., Toohey, D. W., and Brune, W. H.: Dependence of SOA oxidation on organic aerosol mass
570 concentration and OH exposure: experimental PAM chamber studies, Atmos Chem Phys, 11, 1837-
571 1852, DOI 10.5194/acp-11-1837-2011, 2011b.

572 Kang, E., Han, J., Lee, M., Lee, G., Kim, J.C.: Chemical characteristics of size-resolved aerosols from
573 Asian dust and haze episode in Seoul metropolitan city, Atmos. Res., 127, 34-46, 2013.

574 Kessler, S. H., Nah, T., Daumit, K. E., Smith, J. D., Leone, S. R., Kolb, C. E., Worsnop, D. R., Wilson, K.
575 R., and Kroll, J. H.: OH-Initiated Heterogeneous Aging of Highly Oxidized Organic Aerosol, J Phys
576 Chem A, 116, 6358-6365, Doi 10.1021/Jp212131 m, 2012.

577 Kim, Y. J., Woo, J.-H., Ma, Y.-I., Kim, S., Nam, J. S., Sung, H., Choi, K.-C., Seo, J., Kim, J. S., Kang, C.-H.,
578 Lee, G., Ro, C.-U., Chang, D., and Sunwoo, Y.: Chemical characteristics of long-range transport
579 aerosol at background sites in Korea, Atmospheric Environment, 43, 5556-5566, 2009.

580 King, S. M., Rosenoern, T., Shilling, J. E., Chen, Q., Wang, Z., Biskos, G., McKinney, K. A., Pöschl, U.,
581 and Martin, S. T.: Cloud droplet activation of mixed organic-sulfate particles produced by the
582 photooxidation of isoprene, Atmos. Chem. Phys., 10, 3953-3964, 10.5194/acp-10-3953-2010, 2010.

583 Kroll, J. H., and Seinfeld, J. H.: Chemistry of secondary organic aerosol: Formation and evolution of
584 low-volatility organics in the atmosphere, Atmospheric Environment, 42, 3593-3624, DOI
585 10.1016/j.atmosenv.2008.01.003, 2008.

586 Kroll, J. H., Smith, J. D., Che, D. L., Kessler, S. H., Worsnop, D. R., and Wilson, K. R.: Measurement of
587 fragmentation and functionalization pathways in the heterogeneous oxidation of oxidized organic
588 aerosol, Physical Chemistry Chemical Physics, 11, 8005-8014, Doi 10.1039/B905289e, 2009.

589 La, Y.S., Camredon, M., Ziemann, P.J., Valorso, R., Matsunaga, A., Lannuque, V., Lee-Taylor, J., Hodzic,
590 A., Madronich, S., and Aumont, B.: Impact of chamber wall loss of gaseous organic compounds on
591 secondary organic aerosol formation: explicit modeling of SOA formation from alkane and alkene
592 oxidation, Atmos. Chem. Phys., 16, 1417-1431, 2016.
593
594 Lambe, A. T., Ahern, A. T., Williams, L. R., Slowik, J. G., Wong, J. P. S., Abbatt, J. P. D., Brune, W. H.,
595 Ng, N. L., Wright, J. P., Croasdale, D. R., Worsnop, D. R., Davidovits, P., and Onasch, T. B.:
596 Characterization of aerosol photooxidation flow reactors: heterogeneous oxidation, secondary
597 organic aerosol formation and cloud condensation nuclei activity measurements, Atmos Meas Tech,
598 4, 445-461, DOI 10.5194/amt-4-445-2011, 2011.

599 Lambe, A. T., Onasch, T. B., Croasdale, D. R., Wright, J. P., Martin, A. T., Franklin, J. P., Massoli, P.,
600 Kroll, J. H., Canagaratna, M. R., Brune, W. H., Worsnop, D. R., and Davidovits, P.: Transitions from
601 Functionalization to Fragmentation Reactions of Laboratory Secondary Organic Aerosol (SOA)
602 Generated from the OH Oxidation of Alkane Precursors, Environ Sci Technol, 46, 5430-5437, Doi
603 10.1021/Es300274t, 2012.

604 Lambe, A. T., Chhabra, P.S., Onasch,T.B., Brune, W.H., Hunter, J.F., Kroll, J.H., Cummings, M.J., Brogan,
605 J.F., Parmar, Y., Worsnop, D.R., Kolb, C.E., and Davidovits, P.: Effect of oxidant concentration, exposure
606 time and seed particles on secondary organic aerosol chemical composition and yield. Atmos.
607 Chem. Phys.,15, 3063-3075, 2015.
608

609 Lee, M., Song, M., Moon, K. J., Han, J. S., Lee, G., and Kim, K. R.: Origins and chemical characteristics
610 of fine aerosols during the northeastern Asia regional experiment (atmospheric brown cloud east
611 Asia regional experiment 2005), J Geophys Res-Atmos, 112, Artn D22s29 Doi 10.1029/2006jd008210,
612 2007.

613 Lee, T., Choi, J., Lee, G., Ahn, J., Park, J., Atwood, S.A., Schurman, M., Choi, Y., Chung, Y., Collett, Jr. J.L:
614 Characterization of Aerosol Composition, Concentrations, and Sources at Baengnyeong Island, Korea
615 using an Aerosol Mass Spectrometer, Atmospheric Environment 120, 297-306, 2015.
616
617 Li, Z., Li, C., Chen, H., Tsay, S.C., Holben, B., Huang, J., Li, B., Maring, H., Qian, Y., Shi, G., Xia, X., Yin,
618 Y., Zheng, Y., Zhuang, G.: East Asian studies of tropospheric aerosols and their impact on regional
619 climate (EAST-AIRC): An overview, J. Geophys. Re., 116, D00L34, doi:10.1029/2010JD015257, 2011.

620 Lim, S., Lee, M., Kim, S.W., Yoon, S.C., Lee, G., and Lee, Y.J.: Absorption and scattering properties of
621 organic carbon versus sulfate dominant aerosols at Gosan climate observatory in Northeast Asia,
622 Atmos. Chem. Phys., 14, 7781-7793, 2014.
623

624 MaMurry, P.H. and Grosjean, D.: Gas and aerosol wall losses in Teflon film smog chambers, Environ.
625 Sci. Technol., 19(12), 1176-1182, 1985.

626 Massoli, P., Lambe, A. T., Ahern, A. T., Williams, L. R., Ehn, M., Mikkila, J., Canagaratna, M. R., Brune,
627 W. H., Onasch, T. B., Jayne, J. T., Petaja, T., Kulmala, M., Laaksonen, A., Kolb, C. E., Davidovits, P., and
628 Worsnop, D. R.: Relationship between aerosol oxidation level and hygroscopic properties of
629 laboratory generated secondary organic aerosol (SOA) particles, Geophys Res Lett, 37, Artn L24801,
630 Doi 10.1029/2010gl045258, 2010.

631 Mohr, C., DeCarlo, P. F., Heringa, M. F., Chirico, R., Slowik, J. G., Richter, R., Reche, C., Alastuey, A.,
632 Querol, X., Seco, R., Penuelas, J., Jimenez, J. L., Crippa, M., Zimmermann, R., Baltensperger, U., and
633 Prevot, A. S. H.: Identification and quantification of organic aerosol from cooking and other sources
634 in Barcelona using aerosol mass spectrometer data, Atmos Chem Phys, 12, 1649-1665, DOI
635 10.5194/acp-12-1649-2012, 2012.

636 Morgan, W. T., Allan, J. D., Bower, K. N., Esselborn, M., Harris, B., Henzing, J. S., Highwood, E. J.,
637 Kiendler-Scharr, A., McMeeking, G. R., Mensah, A. A., Northway, M. J., Osborne, S., Williams, P. I.,
638 Krejci, R., and Coe, H.: Enhancement of the aerosol direct radiative effect by semi-volatile aerosol
639 components: airborne measurements in North-Western Europe, Atmos Chem Phys, 10, 8151-8171,
640 DOI 10.5194/acp-10-8151-2010, 2010.

641 Ng, N. L., Canagaratna, M. R., Zhang, Q., Jimenez, J. L., Tian, J., Ulbrich, I. M., Kroll, J. H., Docherty, K.
642 S., Chhabra, P. S., Bahreini, R., Murphy, S. M., Seinfeld, J. H., Hildebrandt, L., Donahue, N. M., DeCarlo,

643 P. F., Lanz, V. A., Prevot, A. S. H., Dinar, E., Rudich, Y., and Worsnop, D. R.: Organic aerosol
644 components observed in Northern Hemispheric datasets from Aerosol Mass Spectrometry, Atmos
645 Chem Phys, 10, 4625-4641, DOI 10.5194/acp-10-4625-2010, 2010.

646 Ng, N. L., Canagaratna, M. R., Jimenez, J. L., Chhabra, P. S., Seinfeld, J. H., and Worsnop, D. R.:
647 Changes in organic aerosol composition with aging inferred from aerosol mass spectra, Atmos
648 Chem Phys, 11, 6465-6474, DOI 10.5194/acp-11-6465-2011, 2011.

649 Peltier, R. E., Hecobian, A. H., Weber, R. J., Stohl, A., Atlas, E. L., Riemer, D. D., Blake, D. R., Apel, E.,
650 Campos, T., and Karl, T.: Investigating the sources and atmospheric processing of fine particles from
651 Asia and the Northwestern United States measured during INTEX B, Atmos. Chem. Phys., 8, 1835-
652 1853, 2008.

653 Ramana, M. V., Ramanathan, V., Feng, Y., Yoon, S. C., Kim, S. W., Carmichael, G. R., and Schauer, J. J.:
654 Warming influenced by the ratio of black carbon to sulfate and the black-carbon source, Nat Geosci,
655 3, 542-545, Doi 10.1038/Ngeo918, 2010.

656 Richter, A., Burrows, J. P., Nuss, H., Granier, C., and Niemeier, U.: Increase in tropospheric nitrogen
657 dioxide over China observed from space, Nature, 437, 129-132, 10.1038/nature04092, 2005.

658 Sun, Y. L., Zhang, Q., Schwab, J. J., Chen, W. N., Bae, M. S., Lin, Y. C., Hung, H. M., and Demerjian, K.
659 L.: A case study of aerosol processing and evolution in summer in New York City, Atmos Chem Phys,
660 11, 12737-12750, DOI 10.5194/acp-11-12737-2011, 2011.

661 Takami, A., Miyoshi, T., Shimono, A., Kaneyasu, N., Kato, S., Kajii, Y., and Hatakeyama, S.: Transport of
662 anthropogenic aerosols from Asia and subsequent chemical transformation, J Geophys Res-Atmos,
663 112, Artn D22s31, Doi 10.1029/2006jd008120, 2007.

664 Takegawa, N., Miyakawa, T., Kondo, Y., Jimenez, J. L., Zhang, Q., Worsnop, D. R., and Fukuda, M.:
665 Seasonal and diurnal variations of submicron organic aerosol in Tokyo observed using the
666 Aerodyne aerosol mass spectrometer, J Geophys Res-Atmos, 111, Artn D11206, Doi
667 10.1029/2005jd006515, 2006.

668 Wu, Z. J., Cheng, Y. F., Hu, M., Wehner, B., Sugimoto, N., and Wiedensohler, A.: Dust events in
669 Beijing, China (2004–2006): comparison of ground-based measurements with columnar integrated
670 observations, Atmos. Chem. Phys., 9, 6915-6932, 10.5194/acp-9-6915-2009, 2009.